Numerical Study of Natural Convection in a Square Enclosure Filled by Nanofluid with a Baffle in the Presence of Magnetic Field

Karimdoost Yasuri, Amir*[+]; Izadi, Mohsen; Hatami, Hossein

Department of Mechanical Engineering, Faculty of Engineering, Lorestan University, P.O. Box 465 Khoramabad, I.R. IRAN

ABSTRACT: *Natural convection heat transfer in a square enclosure with a horizontal baffle at the centerline of the left wall containing Al_2O_3-water in the presence of a magnetic field is investigated numerically. The top and bottom horizontal walls are adiabatic. The left wall and the baffle are maintained in constant temperature T_h and the right wall is maintained in constant temperature T_c ($T_c < T_h$). Discretized equations are solved using the SIMPLE algorithm. The numerical simulations have been carried out to determine the effect of parameters in the following ranges: Rayleigh number, $Ra=10^3$ to 10^6, nanoparticles volume fraction between φ =0 to 5%, Hartmann number varied from Ha=0 to 60 and baffle length (L_1=0 to 0.5L). The results show that the heat transfer rate increases with increasing Rayleigh number, but with increasing Hartmann number decreases. Also, increasing the baffle length enhances the heat transfer rate into the enclosure.*

KEYWORDS: *Nanofluid; Natural convection; Baffle; Magnetic field; Al_2O_3-water.*

INTRODUCTION

To save energy and resources and taking into account economic and environmental issues, many research works, over the last few decades, have been carried out to make heat exchange more efficient. The main aim of these investigations is to reduce heat exchanger size needed for a given heat load and to increase the capacity of existing heat exchangers. Interest in studying the mechanisms of fluid flow and heat transfer in an enclosure filled with electrical conductor fluids under the influence of the magnetic field is increasing [1]. A common outcome of these studies is that the fluid in an enclosure that is under magnetic field experiences Lorentz force which affect heat transfer and buoyancy force [2]. A large number of numerical works on natural convection heat transfer have been investigated. *Khanfar et al.* [3] solved numerically the natural convection of a nanofluid in a square enclosure. They investigated the effects of nanoparticles on pure fluids and concluded that with increasing the nanoparticles volume fraction, the heat transfer rate is enhanced. *Aminossadati* and *Ghasemi* [4] performed a study on free convection, by taking a heat source at the bottom of a closed enclosure filled with nanofluid. They investigated the effect of Rayleigh number, location, and geometry of the heater, type and nanoparticles volume fraction on cooling performance. Their results showed that adding nanoparticles to pure water,

* *To whom correspondence should be addressed.*
+ *E-mail: yasuri.am@lu.ac.ir*
1021-9986/2019/5/209-220 *6/$/5.06*

improved cooling performance, especially at low Rayleigh numbers. They found that with the increase of the nanoparticles volume fraction, variations of the average Nusselt number at low Rayleigh numbers, i.e. 10^4 is more than the high Rayleigh number, i.e., 10^5 and 10^6. *Abu-Nada* and *Oztop* [5] studied the effect of inclination angle on natural convection in an enclosure filled with Cu-water nanofluid. They concluded that an inclination angle can be a control parameter for the enclosure filled with nanofluid and also the percentage of heat transfer enhancement using nanoparticles for higher Rayleigh numbers decreases. *Ghasemi et al.* [6] investigated the natural convection of steady laminar nanofluid flow in the presence of a magnetic field in a square enclosure with hot and cold walls in two sides and adiabatic top and bottom walls. They showed that the decrease in the Hartmann number and the increase in the Rayleigh number increase the heat transfer rate. Also, they proved that the heat transfer rate is improved with an increase in the solid volume fraction. *Pirmohammadi* and *Ghassemi* [7] presented a numerical solution of natural convection in a square enclosure with a hot wall in the bottom and cold wall in the top and insulated vertical walls. Their results showed that the inclination angle of the enclosure affect the heat transfer parameters and flow motion. In another numerical study, *Sheikhzadeh et al.* [8] numerically investigated free convection of a TiO_2-water nanofluid in rectangular cavities with differentially heated adjacent walls. They found that when the nanoparticles volume fraction increased, the mean Nusselt number along a hot wall for shallow and tall cavities increased and decreased, respectively. *Xu et al.* [9] carried out an experimental study on free convection heat transfer inside a rectangular enclosure filled molten gallium and subjected to a magnetic field. They showed that the presence of a magnetic field decreases heat transfer. *Hasanuzzaman et al.* [10] considered free convection for a trapezoidal cavity in the presence of a magnetic field with a finite element method and proved that the Nusselt number goes down with magnetic field strength. *Kefayati* [11] carried out Lattice Boltzmann simulation of natural convection in nanofluid-filled 2D long enclosures at the presence of the magnetic field.

Mejri and *Mahmoudi* [12] studied the natural convection in an open cavity with a sinusoidal thermal boundary condition. They found that the heat transfer rate decreases with the rise of Hartmann number and increases with the rise of the Rayleigh number. *Selimefendigil et al.* [13] numerically examined entropy generation due to natural convection in entrapped trapezoidal cavities filled with nanofluid under the influence of the magnetic field. They observed that the averaged heat transfer reduction with the magnetic field is more pronounced at the highest value of the Rayleigh number.

Miroshnichenko et al. [14] have numerically studied natural convection in a partially open trapezoidal cavity filled with a CuO nanofluid under the effect of the uniform magnetic field of various orientations. They have observed that an increase in Hartmann number leads to the heat transfer reduction, while an increase in the nanoparticles, volume fraction reflects the heat transfer enhancement. A numerical analysis of Magnetohydrodynamic natural convection in a wavy open porous tall cavity filled with a Cu–water nanofluid in the presence of an isothermal corner heater was carried out by *Sheremet et al.* [15]. It was found heat transfer enhancement with Rayleigh number and heat transfer reduction with Hartmann number, while the magnetic field inclination angle leads to non-monotonic changes of the heat transfer rate. *Mohebi et al.* [16] have numerically investigated convection heat transfer of Al_2O_3-water nanofluid turbulent flow through internally ribbed tubes with different rib shapes. Their results indicate that the heat transfer increases with nanoparticles volume fraction and Reynolds number but it is accompanied by increasing pressure drop. *Amini et al.* [17] have examined the buoyancy-driven boundary-layer flow from a heated horizontal circular cylinder immersed in water-based alumina (Al_2O_3) nanofluid using variable properties for nanofluid viscosity. They found that with increasing the nanoparticles volume fraction, isotherms become less dense and the absolute values of the stream-function decrease within the domain. Despite a large number of numerical investigations on natural convection of nanofluids inside the enclosure with different boundary conditions, there is no investigation on natural convection with a baffle at the left wall. In the present study, an enclosure with a baffle in the left vertical wall filled nanofluid Al_2O_3-water and subjected to the magnetic field is studied numerically. The effect of various parameters such as baffle length, Hartmann number, Rayleigh number, and nanoparticles volume fraction on heat transfer characteristics is presented.

THEORETICAL SECTION

Model and Governing Equation

Model

Physical model investigated here is a two-dimensional square enclosure with length L filled with nanofluid Al_2O_3-water. The nanofluid is considered steady, incompressible and laminar with constant properties. Upper and lower walls are fully insulated and right and left walls are at Tc and T_h, respectively. A baffle with length L_1 is placed in the middle of the left vertical wall horizontally. A horizontal uniform magnetic field B_o is applied. The schematic diagram of the enclosure is shown in Fig. 1.

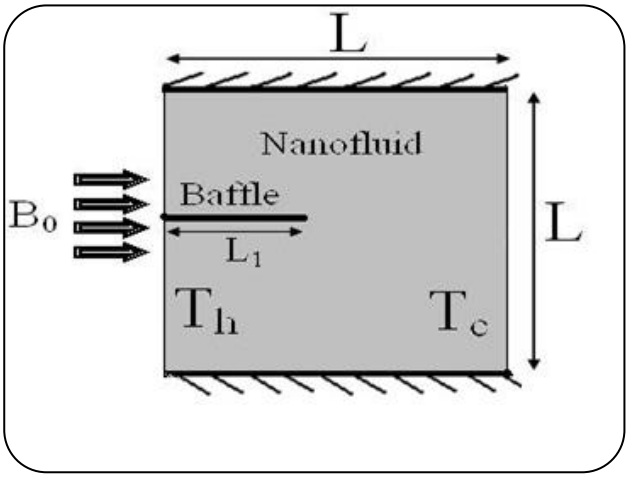

Fig. 1: Schematic depiction of the physical model.

Governing Equations

The flow is assumed to be Newtonian fluid and the density in the buoyancy force is estimated according to Boussinesq approximation. The governing equations are as follows:

Continuity equation

$$\frac{\partial u}{\partial x}+\frac{\partial v}{\partial y}=0 \tag{1}$$

Momentum equations

$$\rho_{nf}\left(u\frac{\partial u}{\partial x}+v\frac{\partial u}{\partial y}\right)=\frac{\partial p}{\partial x}+\mu_{nf}\left(\frac{\partial^2 u}{\partial x^2}+\frac{\partial^2 u}{\partial y^2}\right) \tag{2}$$

$$\rho_{nf}\left(u\frac{\partial u}{\partial x}+v\frac{\partial v}{\partial y}\right)=-\frac{\partial p}{\partial x}+\mu_{nf}\left(\frac{\partial^2 v}{\partial x^2}+\frac{\partial^2 v}{\partial y^2}\right)+$$

$$(\rho\beta)_{nf}\,g(T-T_c)-\sigma_{nf}vB_0^2$$

Energy Equation

$$(\rho C_p)_{nf}\left(u\frac{\partial T}{\partial x}+v\frac{\partial T}{\partial y}\right)=k_{nf}\left(\frac{\partial^2 T}{\partial x^2}+\frac{\partial^2 T}{\partial y^2}\right) \tag{3}$$

Where β is the thermal expansion coefficient, σ is the electrical conductivity, μ is the dynamic viscosity and ρ is the density. Subscript nf denotes the nanofluid. Dimensionless parameters for Equations (1-3) are defined as follows:

$$U=\frac{uL}{\alpha_f},\quad V=\frac{vL}{\alpha_f},\quad X=\frac{x}{L},\quad Y=\frac{y}{L} \tag{4}$$

$$Ra=\frac{g\beta_f L^3(T_h-T_c)}{\nu_f\alpha},$$

$$Pr=\frac{\nu_f}{\alpha_f},\quad \theta=\frac{T-T_C}{T_h-T_C},\quad P=\frac{pL^2}{\rho_{nf}\alpha_f^2},$$

$$Ha=B_0L\sqrt{\frac{\sigma_{nf}}{\nu_f\rho_{nf}}}$$

Where α is the thermal diffusivity, Ha is Hartmann number, Pr is Prandtl number, Ra is Rayleigh number and subscript f means the fluid. The equations of the model in non-dimensional form can be written as:

$$\frac{\partial U}{\partial X}+\frac{\partial V}{\partial Y}=0 \tag{5}$$

$$U\frac{\partial U}{\partial X}+V\frac{\partial U}{\partial Y}=-\frac{\partial P}{\partial X}+\frac{\mu_{nf}}{\rho_{nf}\alpha_f}\left(\frac{\partial^2 U}{\partial X^2}+\frac{\partial^2 U}{\partial Y^2}\right) \tag{6}$$

$$U\frac{\partial U}{\partial X}+V\frac{\partial U}{\partial Y}=-\frac{\partial p}{\partial Y}+\frac{\mu_{nf}}{\rho_{nf}\alpha_f}\left(\frac{\partial^2 V}{\partial X^2}+\frac{\partial^2 U}{\partial Y^2}\right)+$$

$$\frac{(\rho\beta)_{nf}}{\rho_{nf}\beta_f}Ra\,Pr\,\theta-Ha^2\,Pr\,V$$

$$U\frac{\partial \theta}{\partial X}+V\frac{\partial \theta}{\partial Y}=\frac{\alpha_{nf}}{\alpha_f}\left(\frac{\partial^2 \theta}{\partial X^2}+\frac{\partial^2 \theta}{\partial Y^2}\right) \tag{7}$$

The boundary conditions of dimensionless equations are as follows:

$$U=V=0,\quad \frac{\partial\theta}{\partial Y}=0 \qquad \text{On the adiabatic walls} \tag{8}$$

$$U=V=0,\quad \theta=1 \qquad \text{On the left wall and baffle}$$

$$U=V=0,\quad \theta=0 \qquad \text{On the right wall}$$

After solving the equations (5), (6) and (7) using boundary conditions given in equation (8), Nusselt number, which is an appropriate parameter to interpret results, can be determined. The Local Nusselt number along the left hot wall is expressed as

$$Nu_Y = -\frac{k_{nf}}{k_f}\left(\frac{\partial\theta}{\partial X}\right)_{X=0} \quad (9)$$

The average Nusselt number is obtained by integrating the local Nusselt number on constant temperature surfaces. Thermo-physical properties of nanofluid are needed to solve the equations. Density, heat capacity, thermal diffusivity, and thermal expansion coefficient are calculated using properties of base fluid and nanoparticles [18].

$$\rho_{nf} = (1-\varphi)\rho_f + \varphi\rho_p \quad (10)$$

$$(\rho C_p)_{nf} = (1-\varphi)(\rho C_p) + \varphi(\rho C_p)_p$$

$$\alpha_{nf} = k_{nf} \Big/ (\rho C_p)_{nf}$$

$$(\rho\beta)_{nf} = (1-\varphi)(\rho\beta)_f + \varphi(\rho\beta)_p$$

with φ being the solid nanoparticles volume fraction the and subscript p stand for particle. The ratio of electrical conductivity of nanofluid to the electrical conductivity of fluid is obtained as [19]

$$\frac{\sigma_{nf}}{\sigma_f} = 1 + \frac{3\varphi(\sigma_p/\sigma_f - 1)}{(\sigma_p/\sigma_f + 2) - (\sigma_p/\sigma_f - 1)\varphi} \quad (11)$$

Maxwell [19] model is used to calculate the effective thermal conductivity of nanofluid

$$k_{nf} + k_f\left[\frac{(k_p + 2k_f) - 2\varphi(k_f + k_p)}{(k_p + 2k_f) + \varphi(k_f - k_p)}\right] \quad (12)$$

The effective viscosity of nanofluid is modeled according to *Brinkman* equation [20]

$$\mu_{nf} = \mu_f (1-\varphi)^{-2.5} \quad (13)$$

In Table 1, the thermo-physical properties of water and Alumina are provided.

Numerical Approach and Verification of Model

The control volume formulation and the SIMPLE scheme are used to solve the governing equations with the related boundary conditions. A two dimensional uniformly spaced staggered grid system was utilized. The convection-diffusion terms are discretized by a power-law method and the system is numerically modeled in FORTRAN.

To check the validity of developed code in this study, square enclosure with horizontal insulated walls and vertical walls at two different temperatures according to reference [6] is considered and dimensionless temperature on the midline in volume fraction 0.03, Hartman number 30 and Rayleigh numbers 10^3 and 10^5 are depicted in Fig. 2.

The average Nusselt numbers on the hot wall for Hartman number 30 and Rayleigh number 10^4 for various amounts of volume fraction are shown in Table 2.

As can be seen from Fig. 2 and Table 2, a good agreement exists between the results of the present study with those of other works in literature. To ensure a grid-independent solution, the average Nusselt number along the cold wall and the maximum streamline for different grid sizes in volume fraction 0.03, Rayleigh number 10^4, and Hartman number 40 are demonstrated in Table 3.

According to Table 3, it is obvious that the appropriate grid size is 120×120 and it can be observed that Nu_{mc} and $|\psi|_{max}$ remain almost the same for grids finer than this.

RESULTS AND DISCUSSION

To study the strength of convection, Rayleigh number in the range of 10^3 to 10^6 is considered for Ha=30, φ=0.03 and L_1/L=0.5. Isotherms and streamlines for different Rayleigh numbers are plotted in Fig. 3.

As shown in Fig. 3, streamlines near the wall and the baffle are crowded with increasing the Rayleigh number. The reason is the increase of the temperature difference between hot and cold walls that increases flow velocity and therefore streamlines close to the walls are more packed. At Ra=10^3, isotherms in the vicinity of the cold wall are nearly parallel to the wall. The form of isotherms in this condition indicates that at low Rayleigh numbers, heat conduction is dominant. Deformation of isotherms from vertical line to horizontal line at higher Rayleigh numbers demonstrates convection effects. For the relatively large Rayleigh numbers (10^6), isotherms are horizontal that demonstrate the influence of the boundary layer. This behavior reflects the increase of the heat transfer from the enclosure. This consequence can also be seen

Table 1: Thermophysical properties of water and nanoparticles at T=25 °C [4,13].

property	water	Al_2O_3
$\rho(Kg/m^3)$	997.1	3970
C_p (J/Kg.K)	4179	765
K (W/mK)	0.613	40
$\beta\times10^{-5}(1/K)$	21	0.85
$(\Omega.m)^{-1}\sigma$	0.05	10^{-10}

Table 2: Comparison of average Nusselt number of the hot wall.

	φ = 0	φ = 0.02	φ = 0.04
Ghasemi et al. [6]	1.183	1.212	1.249
Present study	1.182	1.215	1.252

Table 3: Average Nusselt number along the cold wall and the maximum streamline for different grids.

Grid	40×40	60×60	80×80	100×100	120×120	140×140
Nu_{mc}	10.099	9.553	9.412	9.410	9.410	9.410
$\lvert\psi\rvert_{max}$	16.855	16.140	16.020	16.017	16.018	16.018

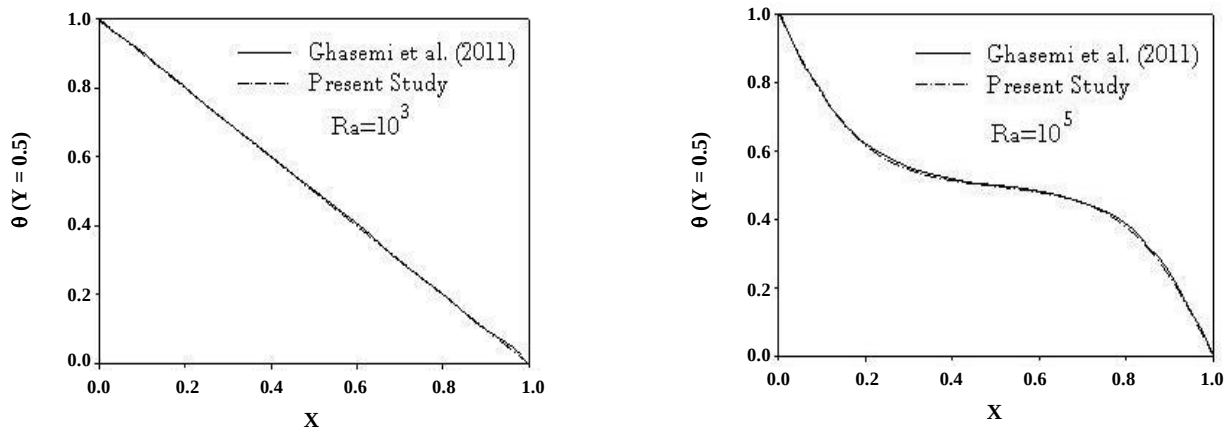

Fig. 2: Comparison of the temperature on the midline between the present results and numerical results by Ghasemi et al. [6].

from the increase of the maximum streamline and Nusselt number of the wall. Fig. 4 shows the local Nusselt number along a hot wall for various Rayleigh numbers.

It is seen that as Rayleigh number increases, Local Nusselt number rises. Also, the temperature gradient close to the baffle decreases and arrives at zero in the hot wall

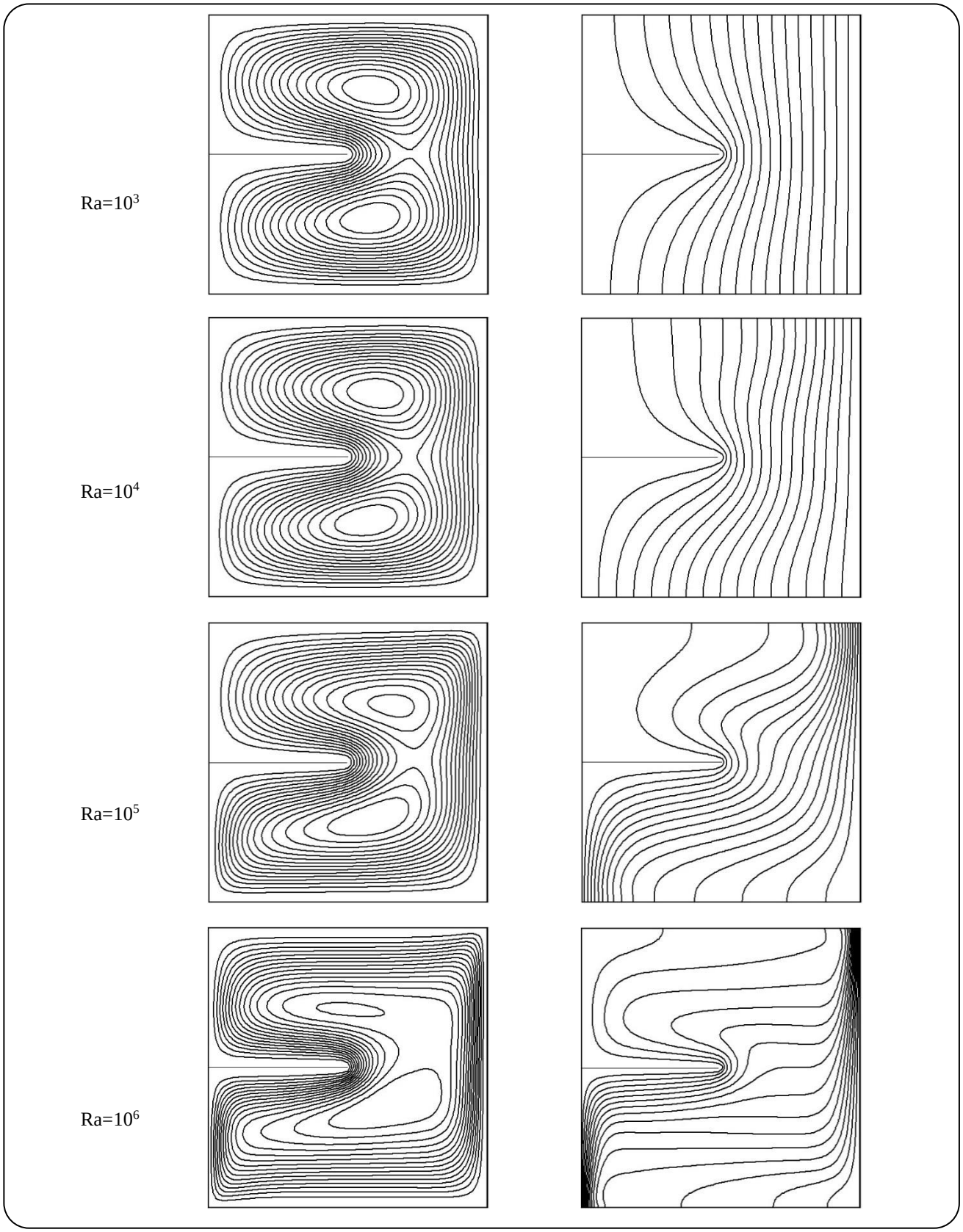

Fig. 3: Isotherms (right) and streamlines (left) for different Rayleigh numbers.

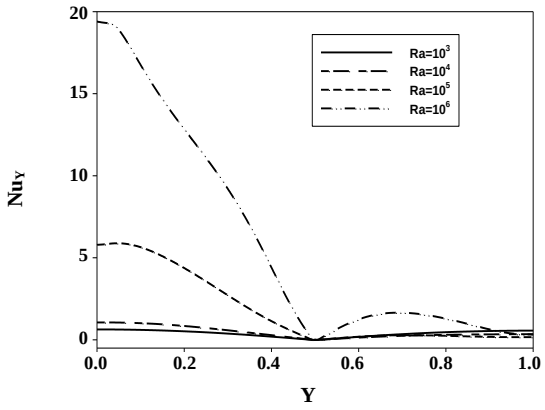

Fig. 4: Local Nusselt number along the hot wall for different Rayleigh numbers.

on the baffle. Fig. 4 presents isotherms and streamlines for different baffle lengths.

As can be seen, isotherms crowd at the cold wall with an increase in the baffle length. Subsequently, the Nusselt number increases. In this issue, two mechanisms affect the behavior of the fluid. The first is the effect of baffle hydrodynamic depending on the baffle length. The second is additional heat which the fluid receives due to the increase of the baffle length. As baffle length increases, contact between the fluid and the hot wall increases and therefore the Nusselt number enhances. On the other hand, with an increase in the baffle length, space for movement of nanofluid inside the enclosure reduces. Therefore, a variation of the maximum Nusselt number and streamline is the consequence of the effect of these two mechanisms. Fig. 6 shows the local Nusselt number along the cold wall.

From Fig.6 we observe that by increasing the baffle length, Nusselt number of cold wall increases which refers to increasing the heat transfer of enclosure. Also, according to Fig. 6 it is evident that in the enclosure without baffles and case of baffle with a length L_1=0.1L, there is little difference in the local Nusselt number, but for the baffle length more than this, the difference is noticeable. Local Nusselt number along the hot wall is demonstrated in Fig. 7.

Unlike Fig. 6 by increasing the baffle length, Nusselt number of the hot wall is reduced due to the increase of the thermal effect of the baffle. Also, in case of the enclosure without baffle and baffle with a length L_1=0.1L, the values of the local Nusselt number are close to each other. But in the middle of the enclosure, a sudden decrease in the amount of local Nusselt number occurs which is due to the presence of the baffle and negligible temperature gradient. It should be noted that the Nusselt number of cold wall is the summation of Nusselt number of hot wall and that of baffle.

Fig. 5 shows isotherms and streamlines for different Hartmann numbers.

As shown, with an increase of Hartmann number, fluid motion and in consequence, the flow velocity decreases inside the enclosure. The reason is that with increasing Hartmann number, Lorentz force, which acts opposite to the flow direction, increases and consequently the flow motion decreases. Since the buoyancy force is more than Lorentz force, the nanofluid motion continues, but its velocity is reduced. Also as seen, with an increase in Hartmann number, the convection and conduction effects are reduced and increased, respectively. The variation of the local Nusselt number on the cold wall is depicted in Fig. 9.

It is observed that with increasing Hartmann number, the convection and therefore the flow velocity is reduced and this results in the decrease of the local Nusselt number. On the other hand, reducing the convection effect, in a situation of constant conduction, Nusselt number decreases. Variation of local Nusselt number of the hot wall is plotted in Fig. 10.

According to Fig. 10 it can be concluded that local Nusselt number decreases with increasing Hartmann number but it is minimized in the center of the enclosure, where baffle is located. Fig. 6 shows isotherms and streamlines of the flow field for different values of the nanoparticles volume fraction.

From Fig. 11, we can see that with varying nanoparticles volume fraction, the overall pattern of streamlines and isotherms do not change, but the increase of the nanoparticles volume fraction with increasing the viscosity of nanofluid results in the reduction of fluid motion. Therefore, heat diffuses into the enclosure from the hot wall. Local Nusselt number along the cold and hot wall for different values of nanoparticles volume fraction is plotted in Fig. 12 and Fig. 13, respectively.

Also, Average Nusselt number along with the cold and the hot wall of the enclosure is provided in Table 4.

As shown in Fig. 12 and Table 4, with an increase of nanoparticles volume fraction, the local and average

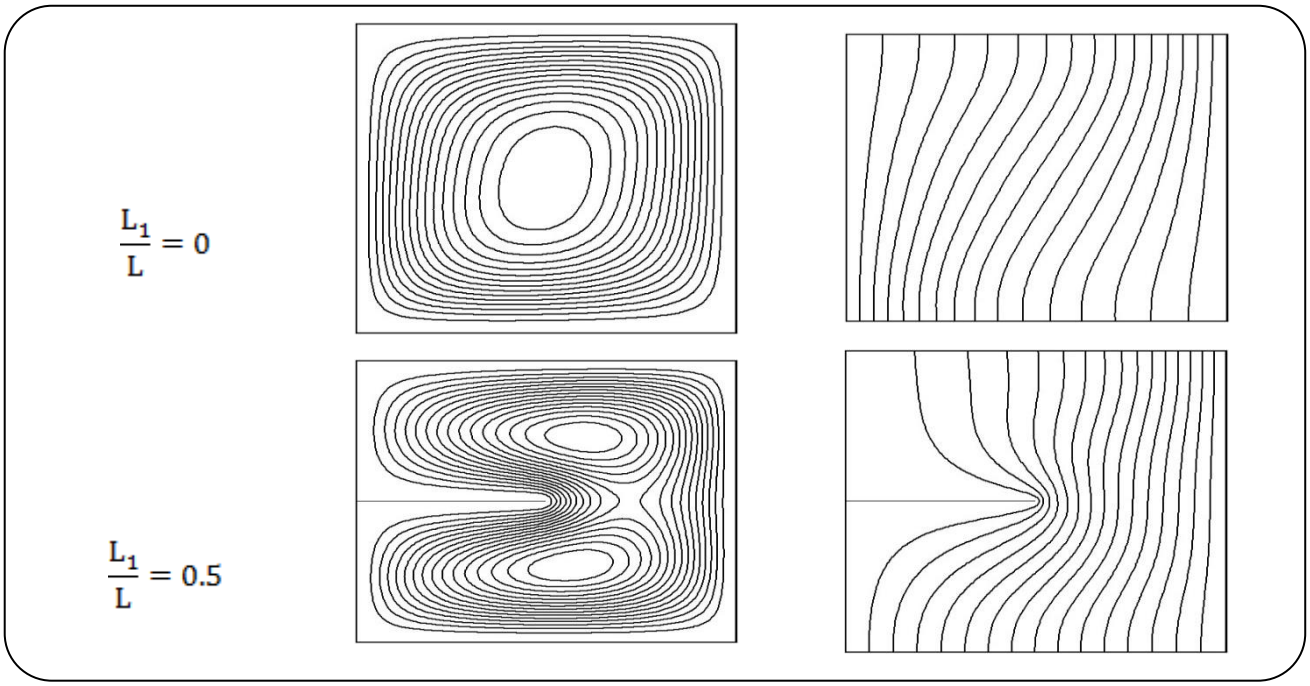

Fig. 4: Isotherms (right) and streamlines (left) for different baffle lengths (L_1).

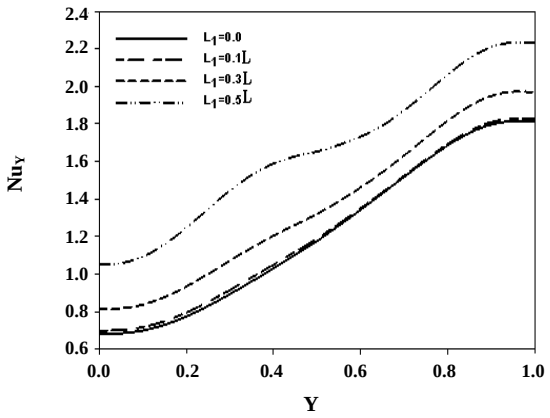

Fig. 6: Local Nusselt number along the cold wall for different lengths of the baffle.

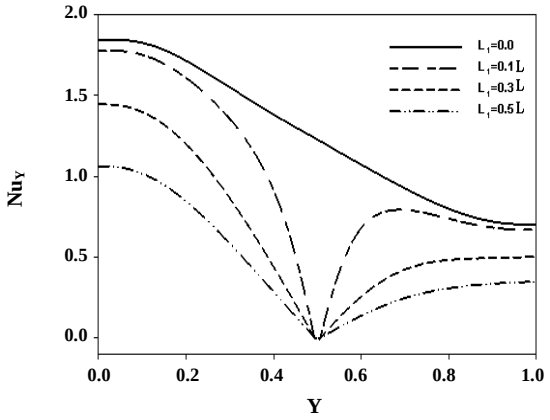

Fig. 7: Local Nusselt number along the hot wall in different lengths of the baffle.

Nusselt number of hot and cold walls and therefore heat transfer rate increases. It should also be noted that increasing nanoparticles volume fraction causes an increase both the heat transfer coefficient and the nanofluid viscosity simultaneously. The increase of the heat transfer coefficient raises the heat transfer rate, while the increase of the viscosity, through reducing the flow velocity of nanofluid results in a reduction in heat transfer. As a result of two effects, the Nusselt number and heat transfer increase.

CONCLUSIONS

This study is focused on the investigation of natural convection in an enclosure with a horizontal thin baffle at the left wall. The most important results of the present numerical study are as follows:

1. Increasing the Rayleigh number increases the flow velocity inside the enclosure by raising the temperature difference between the hot and cold plates. Also, this increase improves the heat transfer of the enclosure and increases the average Nusselt number.

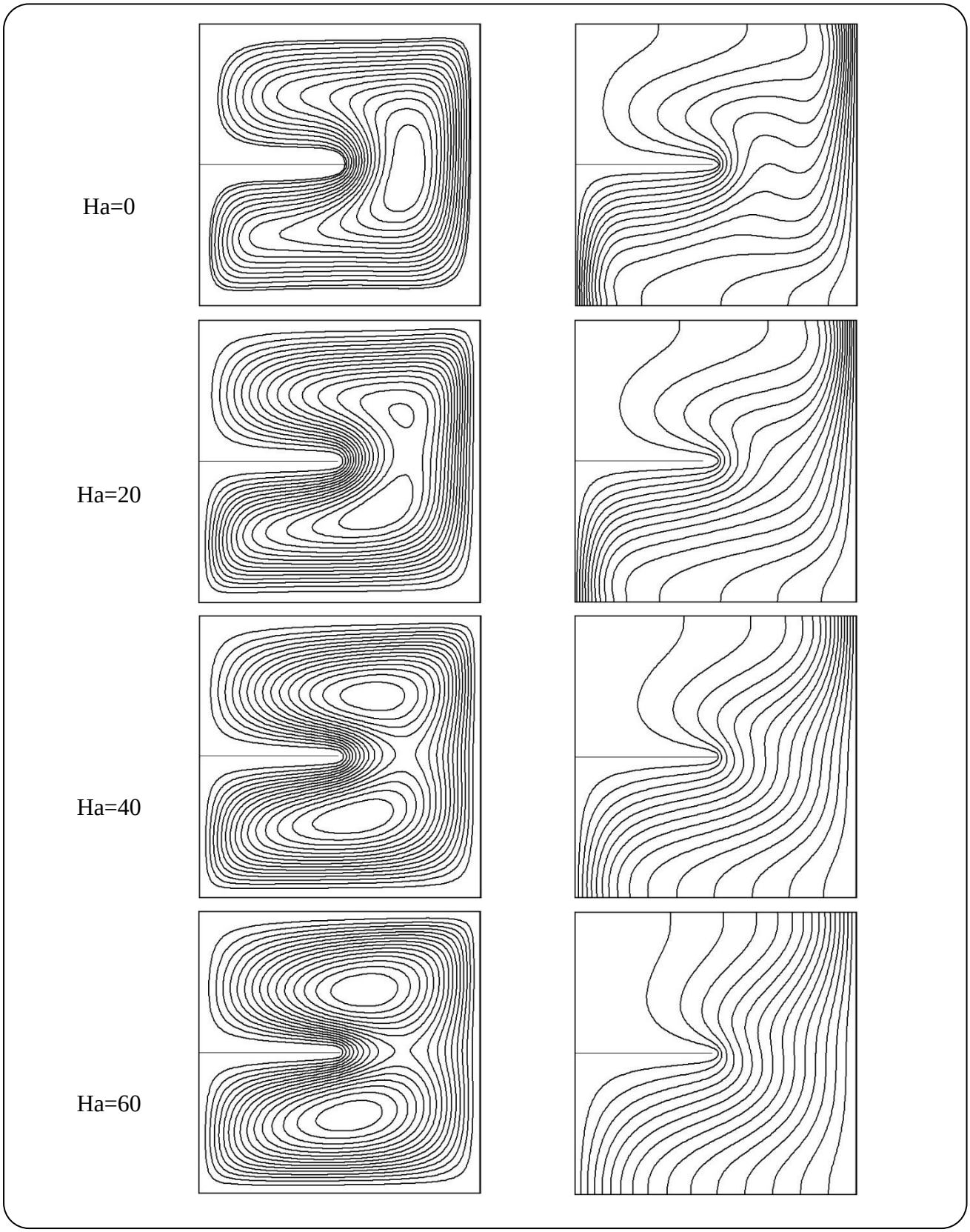

Fig. 5: Isotherms (right) and streamlines (left) for different Hartmann numbers.

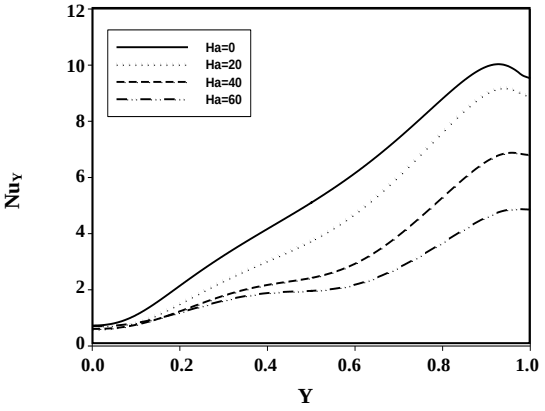

Fig. 9: Local Nusselt number along cold wall for different Hartmann numbers.

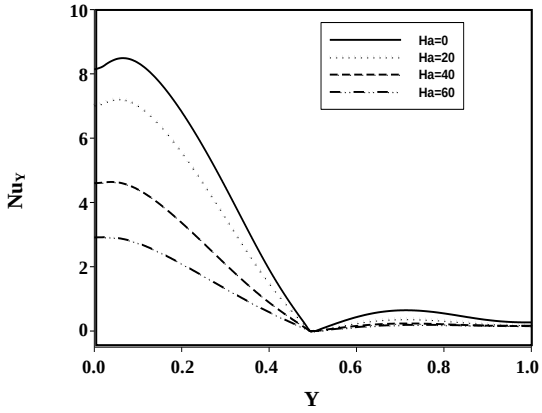

Fig. 10: Local Nusselt number along hot wall for different Hartmann numbers.

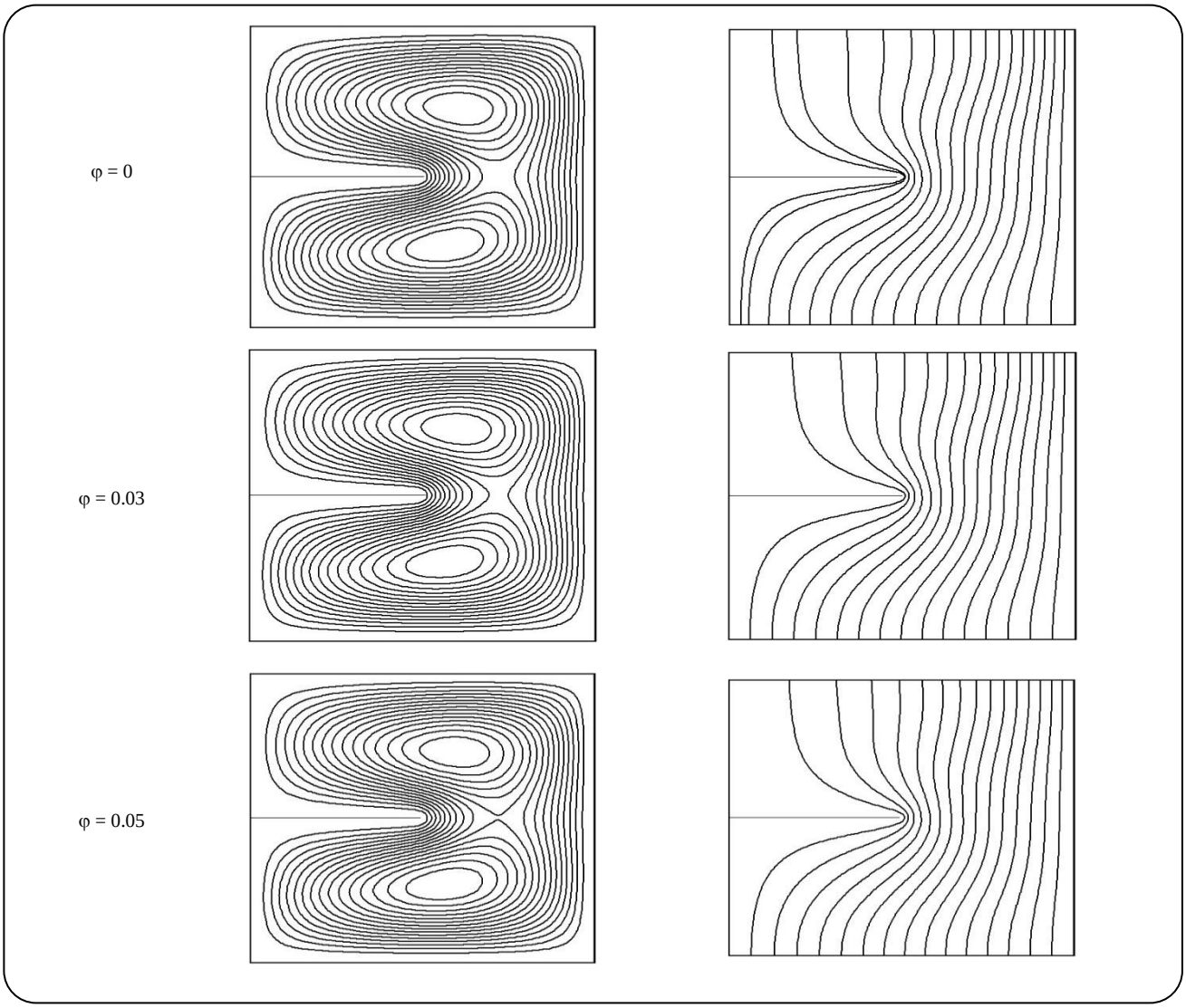

Fig. 6: Isotherms (right) and streamlines (left) for different volume fraction.

Table 4: Average Nusselt number along the cold and hot wall of the enclosure.

φ	0	0.01	0.03	0.05
Nu_{mc}	1.552	1.585	1.654	1.729
Nu_{mh}	0.433	0.438	0.449	0.462

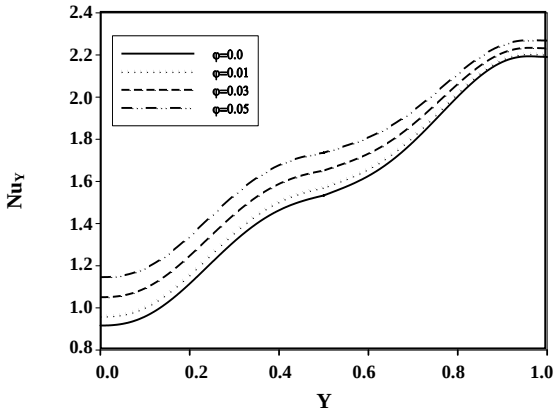

Fig. 12: Local Nusselt number along the cold wall for different volume fractions.

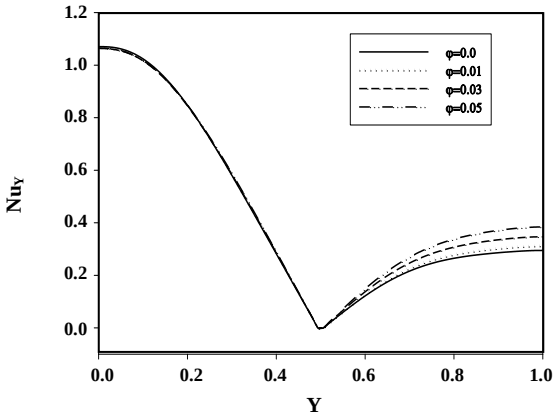

Fig. 13 Local Nusselt number along the hot wall for different volume fractions.

2. By increasing the baffle length, the flow velocity inside the enclosure due to hydrodynamics effects decreases. On the other hand, the contact surface between hot wall and nanofluids increases, therefore the average Nusselt number and subsequently the heat transfer rate increase.

3. With an increase of Hartmann number, flow velocity decreases and therefore the heat transfer rate decreases. So, the flow and heat transfer, through increasing magnetic field strength, can be controlled.

4. Adding nanoparticles to water and increasing the nanoparticles volume fraction increases viscosity, consequently, the flow velocity and thus maximum stream function reduces. However, it improves the heat transfer rate and Nusselt number.

Nomenclature

B_0	Magnetic field strength
Gr	Grashof number
C_p	Specific heat
g	Gravitational acceleration
h	Heat transfer coefficient
Ha	Hartmann number
k	Thermal conductivity
Nu	Nusselt number
p	Pressure
Pr	Prandtl number
Ra	Rayleigh number
T	Temperature
u,v	Velocity component
x,y	Cartesian coordinates

Greek symbols

α	Thermal diffusivity
β	Thermal expansion coefficient
θ	Dimensionless temperature
μ	Dynamic viscosity
ν	Kinematic viscosity
ρ	Density
φ	Volume fraction
ψ	Stream function

Subscripts

c	Cold
f	Fluid
h	Hot
nf	Nanofluid
p	Particle

Received : Mar. 7, 2018 ; Accepted : Aug. 8, 2018

REFERENCES

[1] Ozoe H., Okada K., The Effect of the Direction of the External Magnetic Field on the Three-Dimensional Natural Convection in a Cubical Enclosure, *Int. J. Heat Mass Transfer*, **32**: 1939-1954 (1989).

[2] Garandet J.P., Alboussiere T., Moreau R., Buoyancy Driven Convection in a Rectangular Enclosure with a Transverse Magnetic Field, *Int. J. Heat Mass Transfer*, **35**: 741-748 (1992).

[3] Khanfar K., Vafai K., Lightstone M., Buoyancy-Driven Heat Transfer Enhancement in a Two-Dimensional Enclosure Utilizing Nanofluids, *Int. J. Heat Mass Transfer*, **46**: 3639-3953 (2003).

[4] Aminossadati M.A., Ghasemi B., Natural Convection Cooling of a Localized Heat Source at the Bottom of a Nanofluid-Filled Enclosure, *Eur. J. Mech. B/Fluids*, **28:** 630-640 (2009).

[5] Abu-Nada E., Oztop H.F., Effects of Inclination Angle on Natural Convection in Enclosures filled with Cu-Water Nanofluid, *Int. J. Heat Fluid Flow*, **30**: 669-678 (2009).

[6] Ghasemi B., Aminossadati S.M., Raisi A., Magnetic Field Effect on Natural Convection in a Nanofluid–Filled Square Enclosure, *Int. J. Therm. Sci.*, **50**: 1748-1756 (2011).

[7] Pirmohammadi M., Ghassemi M., Effect of Magnetic Field on Convection Heat Transfer Inside a Tilted Square Enclosure, *Int. Commun. Heat Mass Transfer,* **36**: 776-780 (2009).

[8] Sheikhzadeh G.A., Arefmanesh A., Mahmoodi M., Numerical Study of Natural Convection in a Differentially-Heated Rectangular Cavity Filled with TiO_2-Water Nanofluid, *J. Nano Res.*, **13**: 75-80 (2011).

[9] Xu B., Li B.Q., Stock D.E., Nithyadevi N., An Experimental Study of Thermally Induced Convection of Molten Gallium in Magnetic Field, *J. Heat Mass Transfer*, **49**: 2009-2019 (2006).

[10] Hasanuzzaman M., Rahman Oztop H.F., Rahim M., Saidur N.R., Varol Y., Magnetohydrodynamic Natural Convection in Trapezoidal Cavities, *Int. Commun. Heat Mass Transf.*, **39**: 1384-1394 (2012).

[11] Kefayati Gh.R., Lattice Boltzmann Simulation of Natural Convection in Nanofluid-Filled 2D Long Enclosures at Presence of Magnetic Field, *Theor. Comput. Fluid Dyn.*, **27**(6): 865–883 (2013).

[12] Mejri I., Mahmoudi A., MHD Natural Convection in a Nanofluid-Filled Openenclosure with a Sinusoidal Boundary Condition, *Chem. Eng. Research Design*, **98**: 1–16 (2015).

[13] Selimefendigil F., Öztop H.F., Abu-Hamdeh N., Natural Convection and Entropy Generation in Nanofluid Filled Entrapped Trapezoidal Cavities under the Influence of Magnetic Field, *Entropy*, **18**: 43-53 (2016).

[14] Miroshnichenko I.V., Sheremet M.A., Oztop H.F., Al-Salem K., MHD Natural Convection in a Partially Open Trapezoidal Cavity Filled with a Nanofluid, *Int. J. Mech. Sci.*, **119:** 294–302 (2016).

[15] Sheremet M.A., Oztop H.F., Pop I., Al-Salem K., MHD Free Convection in a Wavy Open Porous Tall Cavity Filled with Nanofluids under an Effect of Corner Heater, *Int. J. Heat Mass Transfer*, **103:** 955–964 (2016).

[16] Mohebbi K., Rafee R., Talebi F., Effects of Rib Shapes on Heat Transfer Characteristics of Turbulent Flow of Al_2O_3-Water Nanofluid inside Ribbed Tubes, *Iran. J. Chem. Chem. Eng. (IJCCE)*, **34** (3): 61-77 (2015).

[17] Habibi M.R., Amini M., Arefmanesh A., Ghasemikafrudi E., Effects of Viscosity Variations on Buoyancy-Driven Flow from a Horizontal Circular Cylinder Immersed in Al_2O_3-Water Nanofluid, *Iran. J. Chem. Chem. Eng. (IJCCE)*, Articles in Press, Accepted Manuscript, Available Online from 07 February (2018).

[18] Sheikholeslami M., Gorji Bandpy M., Ellahi R., Mohsan H., Soheil S., Effects of MHD on Cu–Water Nanofluidflow and Heat Transfer by Means of CVFEM, *J. Magnetism Magnetic Materials*, **349**: 188-200 (2014).

[19] Maxwell, J. C., "A treatise on Electricity and Magnetism", Oxford University Press, Cambridge, 2nd ed., 435-441 (1904).

[20] Brinkman, H. C., The Viscosity of Concentrated Suspensions and Solution, *J. Chem. Phys.*, **20**: 571–581 (1952).